ELSEVIER

Journal of Alloys and Compounds 404–406 (2005) 682–686

Journal of ALLOYS AND COMPOUNDS

www.elsevier.com/locate/jallcom

Electrochemical properties of nanocrystalline Mg_2Ni-type alloys prepared by mechanical alloying

S. Bliznakov[b], N. Drenchev[a], B. Drenchev[a], P. Delchev[a], P. Solsona[a,c], T. Spassov[a,*]

[a] *Department of Chemistry, University of Sofia "St.Kl.Ohridski", 1126 Sofia, Bulgaria*
[b] *Central Laboratory of Electrochemical Power Sources, Bulgarian Academy of Sciences, Sofia, Bulgaria*
[c] *Departament de Física, Universitat Autonoma de Barcelona, LMT, 08193 Bellaterra, Spain*

Received 18 June 2004; received in revised form 24 January 2005; accepted 31 January 2005
Available online 3 August 2005

Abstract

The electrochemical hydrogen charge/discharge properties of nanocrystalline and nanocrystalline/amorphous Mg_2Ni-based alloys with different microstructure (e.g. different average nanocrystals size, different amount of the amorphous phase), prepared by mechanical alloying and mechanical alloying with subsequent controlled annealing, were studied. It was found that larger amount of amorphous phase improved the capacity of the alloy. Alloys with similar nanograin size, but prepared in a different way showed different electrochemical charge/discharge behaviour as well. The as-milled nanocrystalline alloy (7–10 nm), characterized by higher concentration of defects and some amorphous fraction, reveals slightly higher hydrogen capacity than the completely nanocrystalline material (7–10 nm), produced by milling and subsequent annealing. The nanocrystal size reduction in fully crystalline alloys results in noticeable increase of the hydrogen capacity as well.
© 2005 Elsevier B.V. All rights reserved.

Keywords: Mg–Ni alloys; Nanocrystalline; Mechanical alloying; Electrochemical properties

1. Introduction

Mg–Ni alloys are considered as the most promising materials for hydrogen storage and energy conversion due to their high hydrogen storage capacity, low cost and light weight. Their slow hydriding/dehydriding kinetics at room temperature and rapid degradation in alkaline solution and therefore relatively low discharge capacity limit their practical application as anode materials (MH) in a rechargeable battery. Mechanical milling (MM) and mechanical alloying (MA) were shown to be very effective ways to increase the hydrogen discharge capacity as well as to improve the characteristics of a negative MH electrode [1,2], modifying the microstructure and the surface of the material. The improved properties are mainly explained by the appropriate nano-/amorphous microstructure, which facilitates the hydrogen diffusion process and the charge transfer reaction and leads to high electrochemical capacity [3]. Alloying (e.g. partial substitution of Al, V, Zr and Ti for Mg) is another approach to improve the electrode characteristics of ball-milled Mg–Ni alloys [2–7].

Although a number of studies on the electrode characteristics of mechanically alloyed Mg_2Ni-based alloys have been already reported [1–3,5–12], the results are very often inconsistent and the influence of the microstructure on the electrochemical properties is not thoroughly investigated.

In our recent works [13,14] preparation of nanocrystalline and nano-/amorphous Mg_2Ni-based alloys by MA and MA with subsequent annealing was reported. Improved hydrogen sorption kinetics in nanocrystalline $Mg_{1.9}(Ti,Zr)_{0.1}Ni$ from hydrogen gas phase compared to nanocrystalline Mg_2Ni was observed. Therefore, the goal of the present work was to produce nanocrystalline and nanocrystalline/amorphous $Mg_{1.9}(Ti,Zr)_{0.1}Ni$ alloys with a controlled grain size and amount of amorphous phase (by mechanical alloying and mechanical alloying with subsequent controlled annealing) and study the influence of the microstructure on their electrochemical hydrogen charge/discharge properties.

* Corresponding author. Tel.: +359 2 627838; fax: +359 2 9625438.
E-mail address: tspassov@chem.uni-sofia.bg (T. Spassov).

0925-8388/$ – see front matter © 2005 Elsevier B.V. All rights reserved.
doi:10.1016/j.jallcom.2005.01.125

2. Experimental

Pure elemental powders of magnesium, nickel, titanium and zirconium were used as starting materials. The ball milling was performed with a planetary-type mill (Fritsch P5) under pure argon gas atmosphere with a rotation speed of 300 rpm, ball to powder mass ratio (B/P) of 15/1 under hydrogen gas atmosphere of 5 atm. Stainless steel vials and mill were used. The samples were handled in a glove box under Ar. Small amount of the powder was taken from the mill at certain periods of time for structural, morphological and thermal analysis. Controlled annealing of the as-milled alloys in a protective Ar gas atmosphere was carried out in order to achieve certain nanostructure.

The powder morphology and the microstructure of the alloys treated under different milling and annealing conditions were analysed by X-ray diffraction (XRD) using a Cu Kα radiation and scanning electron microscopy (JEOL 5510 SEM). The X-ray diffraction data were analysed by a full pattern fitting procedure (Rietveld method) using the program MAUD [15] and the lattice parameters, the amount of the different phases, the crystallite size and the internal strain were determined.

Some of the powders were treated in a 0.1 mol/l NH_4F for 30 min at room temperature. The pH value of the fluorination solution undergoes a big change from acid to alkaline during the sample treatment. The fluorinated powders were dried at about 50 °C in air.

The electrochemical measurements were realized by a three electrode cell. The working electrodes were made by mixing the alloy powder and Ni powder (in a weight ratio 1:3) and 5% polyvinyl alcohol solution (PVA). Then the mixture was pasted on a nickel foam sheet (about 1 cm^2) and after drying was pressed at about 150 atm. $NiOOH/Ni(OH)_2$ was used as counter electrode and Hg/HgO—as reference electrode. In the charge/discharge cycles each electrode was charged for 10–50 h at 1–10 mA/cm^2 (or 10–100 mA/g alloy) and discharged to -0.6 V versus Hg/HgO at different current densities in a 6 M KOH water solution.

3. Results

3.1. Formation of nano-Mg_2Ni-based alloys by BM and by BM with subsequent annealing

SEM observations reveal that after continuous milling the powder particles are in the range of 1–10 μm and relatively homogeneous in size, Fig. 1. Some smaller particles, cold welded together, can be also seen. The energy dispersive analysis (EDX) analysis indicates that Mg and Ni, as well as the alloying elements (Ti, Zr) are uniformly distributed in the powder mixture.

Typical XRD patterns of $Mg_{1.9}Ti_{0.05}Zr_{0.05}Ni$ alloys produced by ball milling at different milling times are shown in Fig. 2. It is seen that after sufficient time of milling

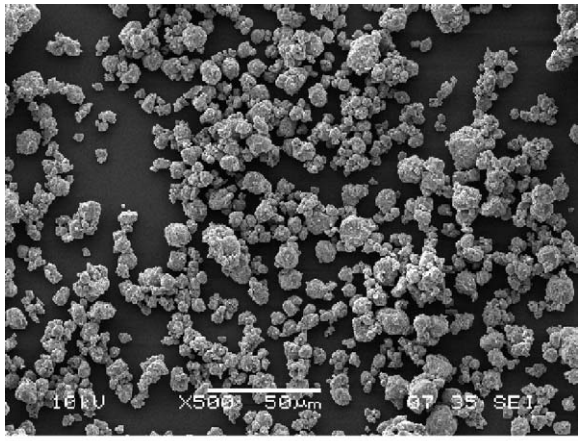

(a)

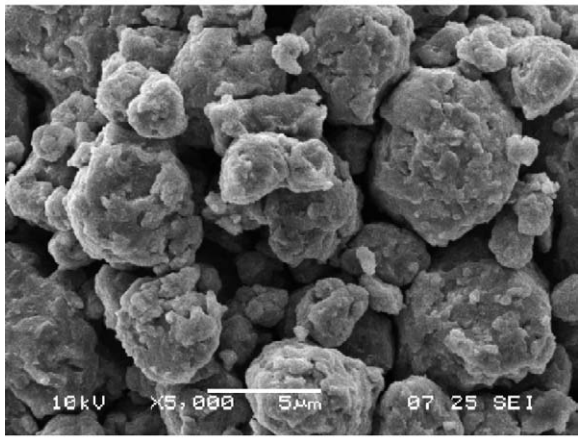

(b)

Fig. 1. SEM micrographs of mechanically alloyed $Mg_{1.9}Ti_{0.05}Zr_{0.05}Ni$.

(17–24 h) the powders reveal nanocrystalline/amorphous microstructure, consisting of mainly hexagonal Mg_2Ni phase. At these concentrations (3.at.%) the alloying elements (Ti, Zr) form solid solutions, most probably substituting Mg in the crystal lattice of the Mg_2Ni phase [13]. Our recent TEM study confirmed that the particles consist of nanocrystals and

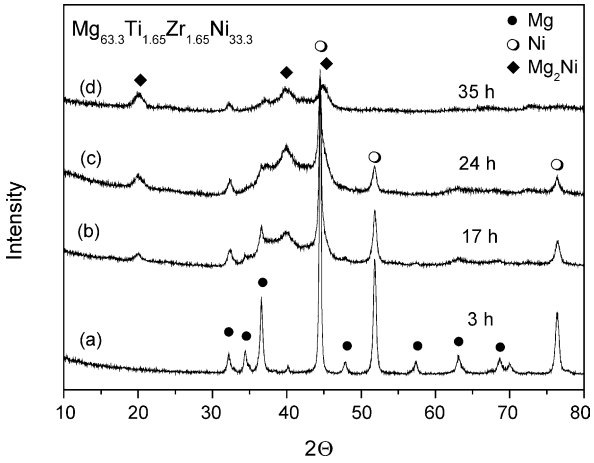

Fig. 2. XRD patterns of $Mg_{1.9}Ti_{0.05}Zr_{0.05}Ni$ as a function of milling time.

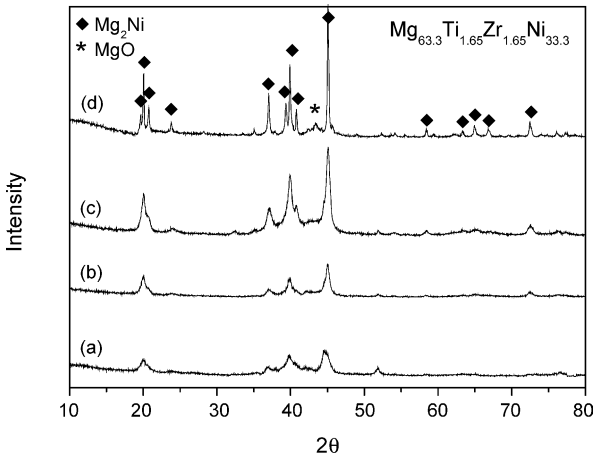

Fig. 3. XRD patterns of ball-milled $Mg_{1.9}Ti_{0.05}Zr_{0.05}Ni$ after different heat treatments: 10 min at 200 °C (a), 10 min at 350 °C (b), 1 h at 350 °C (c), and 1 h at 500 °C (d).

small amount of amorphous (disordered) phase around the nanocrystals [14]. It was reported that the time to reach certain amorphous fraction depends strongly on the milling intensity as well as on the contamination of the milling atmosphere [13,14]. Ball milling to amorphous material and subsequent annealing (in the temperature range of 200–400 °C) leads to nanocrystalline Mg_2Ni-based alloys (10–20 nm), Fig. 3. Continuous milling of the elemental powders (>30 h) leads to the formation of completely nanocrystalline alloy with grain size of about 7–10 nm. Further milling does not change noticeably the microstructure. Generally, varying the milling time and temperature of annealing (after milling) different microstructures of the Mg_2Ni-based alloys could be obtained in a controlled way, Fig. 3.

The thermal stability of the nanocrystalline Mg_2Ni microstructures produced by BM or BM with low temperature annealing was also studied. Annealing at 350 °C for 1 h leads to a nanocrystals growth from 7–10 to about 15–20 nm, Fig. 3 (curves b and c). Substantial grain growth was observed at temperatures above 450 °C, which is far above the usual temperatures of H-desorption for these materials, Fig. 3 (curve d).

3.2. Electrochemical properties (cycle life measurements)

Cyclic voltammetry (CV) curves at two different temperatures of the nanocrystalline Mg_2Ni-based alloy (crystallite size of 7–10 nm, without amorphous phase) at scanning rate of 10 mV/s are shown in Fig. 4. Both anodic oxidation and cathodic reduction peaks can be seen, as the current density of the anodic oxidation peak slightly increases with the temperature, indicating an improvement of the electrochemical hydrogen desorption kinetics. This result also shows that the solid-state hydrogen diffusion process has an influence on the overall electrochemical hydrogen sorption capability of the material studied.

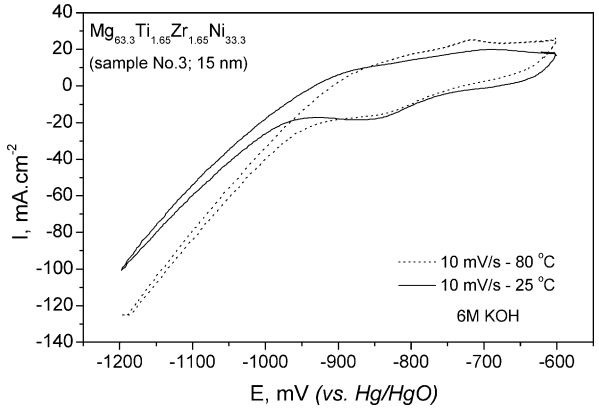

Fig. 4. Voltammograms (CV curves) of nanocrystalline $Mg_{1.9}Ti_{0.05}Zr_{0.05}Ni$ alloy at two different temperatures (scan rate 10 mV/s).

Electrochemical charge/discharge characteristics of $Mg_{1.9}(Ti,Zr)_{0.1}Ni$ alloys with different microstructure at constant current density for the first charge/discharge cycle are presented in Fig. 5. The first discharge curves do not show a clear plateau, which is an indication for an amorphous or extremely fine nanocrystalline microstructure and for the absence of a well-defined boundary between hydrided and non-hydrided regions in the alloy. Generally, the discharge capacities measured for the alloys studied were low and increase with decreasing the discharge current. As it was mentioned in the introduction the results on the electrochemical characteristics (discharge capacity, cycle life stability) of Mg_2Ni-based alloys available in the literature substantially differ from each other. Most of the studies [1–3] reveal low discharge capacity and unsatisfactory cycle life stability, although some higher hydrogen discharge capacities, about 300–500 mAh/g, are also shown [5,6]. The higher initial capacity of the Mg-based alloys however decreases strongly after the first 2–3 cycles [1,2,5,6]. The capacities in the present study are close to those of the previous works on the electrochemical behaviour of Mg_2Ni-based alloys, obtained after the first 1–2 charge/discharge cycles [1,2,5,6].

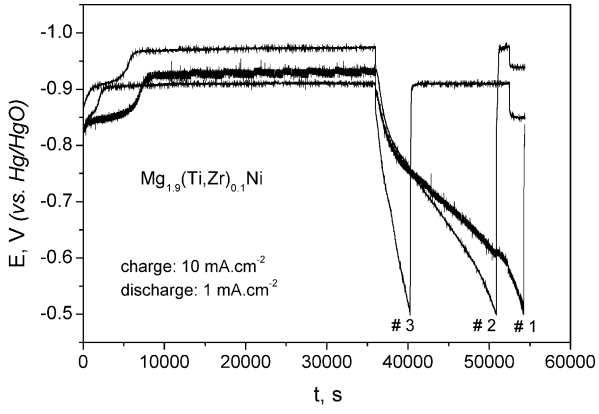

Fig. 5. Initial charge/discharge curves at galvanostatic conditions of $Mg_{1.9}Ti_{0.05}Zr_{0.05}Ni$ alloys with different nanostructures: #1: nanocrystalline (7–10 nm) + amorphous fraction (∼10%), #2: nanocrystalline (7–10 nm), #3: nanocrystalline (∼15 nm).

Preliminary fluorination of the alloy powder with NH_4F (causing formation of MgF_2 on the surface of the particles) does not lead to essential change in the discharge capacity and cycle life due to the low stability of the MgF_2 in strong alkaline water solutions (6 M KOH) and rapid $Mg(OH)_2$ formation. An influence of the pressure of the electrode preparation on the charging/discharging process was found, as generally lower pressure improves the capacity. Systematic study of the above dependence is however still necessary for the optimization of the electrode preparation technique.

4. Discussion

Although the discharge capacities were found to be generally low (below 60–65 mAh/g) a marked difference between the initial discharge behaviour of the different microstructures is observed with a very good reproducibility. The discharge curves presented in Fig. 5 correspond to a nanocrystalline $Mg_{1.9}(Ti,Zr)_{0.1}Ni$ alloy in three different microstructural states: sample no. 1 is nanocrystalline (7–10 nm), obtained by BM and contains some amorphous fraction (about 10%), sample no. 2 is completely nanocrystalline, prepared by BM and subsequent low temperature annealing to fully nanocrystalline state (grain size of about 7–10 nm) and sample no. 3 is completely nanocrystalline, prepared by BM and subsequent annealing (350 °C) to obtain fully nanocrystalline state with larger grain size (∼ 15 nm) compared to sample no. 2. The alloy with the finest microstructure (no. 1) shows the highest discharge capacity and this with the coarsest (no. 3)—the lowest. Comparing the discharge curves of the sample nos. 3 and 2 the influence of the nanograin size on the discharge capacity can be seen in a clear way, because both samples are produced by BM for the same milling time and are later annealed to a different grain size. This result is in agreement with previous studies [9,16], proving that refining the grain size by BM improves the discharge capacity of Mg_2Ni-based alloys. Our study, however, extends the validity of this finding to much finer microstructures (<10–15 nm) compared to the grain size of the works cited above, where the microstructures studied are characterized with average grain size above 50 nm. Another interesting comparison can be made between sample nos. 1 and 2. XRD analysis reveals that both samples, produced by BM, have the same average grain size of about 7–10 nm, but the sample no. 2 is later annealed at low temperature (200 °C) just for reducing the internal strain and of the disordered phase in the grain boundaries produced by BM, without noticeable grain growth to occur. Although the difference in the discharge capacities of the last two samples is not big, the as-milled alloy (containing some amorphous fraction and internal strain) shows a higher value. Our previous hydrogen absorption/desorption study [13] also showed that the nano-/amorphous $Mg_{1.9}M_{0.1}Ni$ (M = Ti, Zr, V) alloys produced by continuous milling possess improved H-sorption kinetics (in hydrogen gas phase) compared to the coarser nanocrystalline Mg_2Ni.

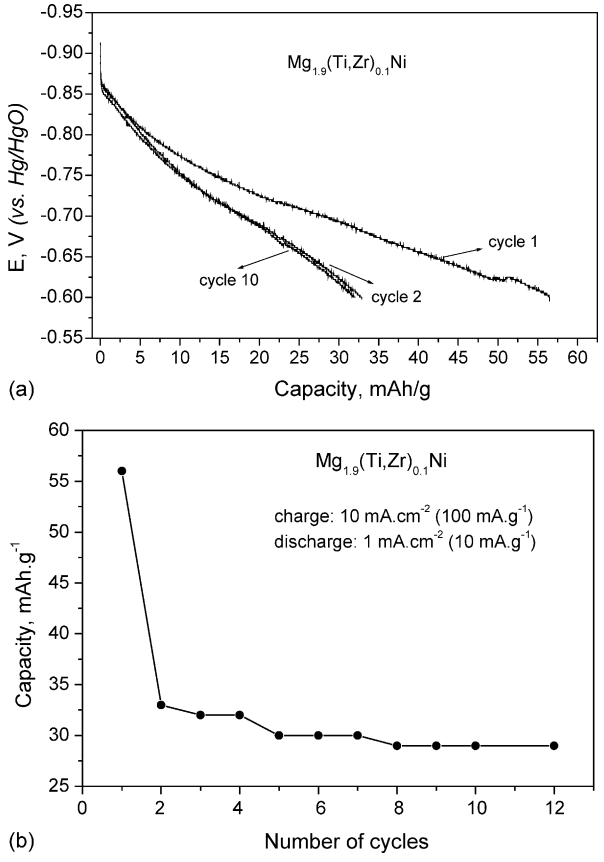

Fig. 6. Cycle behaviour of $Mg_{1.9}Ti_{0.05}Zr_{0.05}Ni$ (a) and Discharge capacity as a function of the cycle number (sample no. 1).

The electrochemical cycling behaviour of nanocrystalline $Mg_{1.9}(Ti,Zr)_{0.1}Ni$ alloy (<10 nm) produced just by ball milling is shown in Fig. 6. After initial fast degradation the discharge capacity takes a constant value of about 30 mAh/g. As it was already mentioned similar degradation of the discharge capacity with cycle number of MA Mg-based amorphous alloys was observed in most of the previous works [1,2,5,6].

Although, because of blocking the particles surface, due to the formation of mainly $Mg(OH)_2$, the entire volume of the material could not be hydrided electrochemically, from the shape of the discharge curves three different "plateaus" can be distinguished (Figs. 5 and 6(a)), which can be associated with the three different microstructural elements in the alloy studied defined by Orimo and Fujii [16] and proved in our previous studies [17,18] as: nanograins, interface between the grains and amorphous phase. For the samples in completely crystalline state only two plateaus were observed, due to the lack of amorphous phase.

5. Conclusion

The influence of the microstructure of nanocrystalline Mg_2Ni-based alloys (with different nanocrystal size,

different amount of amorphous phase) on their electrochemical hydrogen capacity and cycle stability was investigated. Larger amount of amorphous phase was found to improve the capacity of the nanocrystalline/amorphous alloys studied. The as-milled nanocrystalline alloy (7–10 nm), containing some amorphous fraction and internal strain, shows a higher discharge capacity compared to the completely nanocrystalline material (7–10 nm), prepared by ball-milling and subsequent annealing. Reducing the nanocrystal size in fully crystalline alloys results in noticeable increase of the hydrogen capacity as well.

Acknowledgements

The work has been supported by the EU HPRN-CT-2002-00208. SEM analysis was carried out by JEOL 5510 SEM, donated of Sofia University (T.S.) by the Alexander von Humboldt Foundation, Germany.

References

[1] H. Niu, D.O. Northwood, Int. J. Hydrogen Energy 27 (2002) 69–77.
[2] H. Yuan, Q. Li, H. Song, Y. Wang, J. Liu, J. Alloys Compd. 353 (2003) 322–326.
[3] S.S. Han, H.Y. Lee, N.H. Goo, W.T. Jeong, K.S. Lee, J. Alloys Compd. 330–332 (2002) 841–845.
[4] S.-Ch. Han, P.S. Lee, J.-Y. Lee, A. Zuettel, L. Schlapbach, J. Alloys Compd. 306 (2000) 219–226.
[5] N. Cui, J.L. Luo, K.T. Chuang, J. Alloys Compd. 302 (2000) 218–226.
[6] H.Y. Lee, N.H. Goo, W.T. Jeong, K.S. Lee, J. Alloys Compd. 313 (2000) 258–262.
[7] M. Pasturel, J.-L. Bobet, B. Chevalier, J. Alloys Compd. 356–357 (2003) 764–767.
[8] S.-I. Yamaura, H.-Y. Kim, H. Kimura, A. Inoue, Y. Arata, J. Alloys Compd. 339 (2002) 230–235.
[9] M. Zhu, Z.M. Wang, C.H. Peng, M.Q. Zeng, Y. Gao, J. Alloys Compd. 349 (2003) 284–289.
[10] T. Kuji, H. Nakano, T. Aizawa, J. Alloys Compd. 330–336 (2002) 590–596.
[11] X.P. Gao, F.X. Wang, Y. Liu, G.L. Pan, S. Li, J.Q. Qu, F. Wu, H.T. Yuan, D.Y. Song, J. Electochem. Soc. 149 (12) (2002) A1616–A1619.
[12] S.-I. Yamaura, H.-Y. Kim, H. Kimura, A. Inoue, Y. Arata, J. Alloys Compd. 339 (2002) 230–235.
[13] P. Solsona, S. Doppiu, T. Spassov, S. Suriñach, M.D. Baró, J. Alloys Compd. 381 (2004) 66–71.
[14] T. Spassov, P. Solsona, S. Bliznakov, S. Suriñach, M.D. Baró, J. Alloys Compd. 356–357 (2003) 639–643.
[15] L. Lutterotti, S. Gialanella, Acta Mater. 46 (1997) 101.
[16] S. Orimo, H. Fujii, Appl. Phys. A 72 (2001) 167–186.
[17] T. Spassov, U. Köster, J. Alloys Compd. 279 (1998) 279.
[18] T. Spassov, L. Lyubenova, U. Koster, M.D. Baro, Mater. Sci. Eng. A 375–377 (2004) 794.